

Transition crossing of proton beams in SIS100

Longitudinal beam dynamic simulations including space charge

Thilo Egenolf

GSI Helmholtzzentrum für Schwerionenforschung GmbH,
Planckstrasse 1, 64291 Darmstadt, Germany

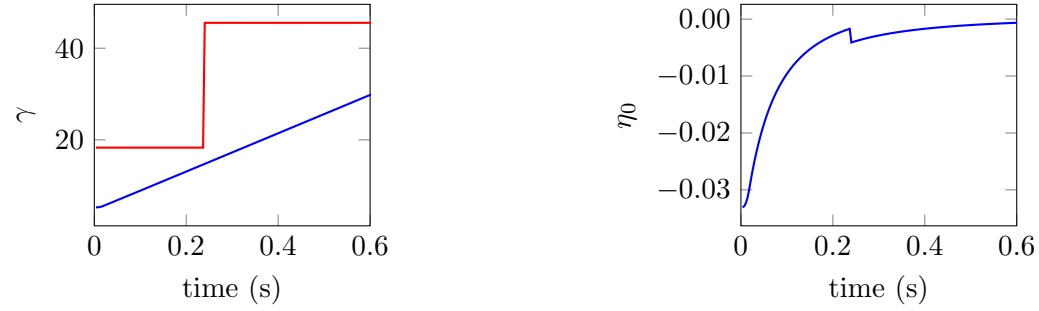
February 7, 2023

The proton cycle in the SIS100 synchrotron is designed to deliver single bunches with 2×10^{13} particles at 29 GeV. During the cycle beam dynamics near transition energy have to be analyzed to avoid an significant emittance blow-up. In the past two scenarios were discussed, a shift of the transition energy above the extraction energy and a transition crossing with a so called γ_t jump. To estimate the possible emittance blow-up in both scenarios, longitudinal simulations are presented including the Johnsen effect based on the second order phase slip factor and the effect of longitudinal space charge. Furthermore, different parameters in the design of the γ_t jump are varied and a set of parameters is proposed that shows minimal longitudinal emittance growth in the simulations.

1 Introduction

In order to reach the desired SIS100 extraction energy crossing or changing the transition energy is necessary during the acceleration cycle. In the SIS100 Project Note "Overview of the Longitudinal Beam Dynamics for the SIS100 Proton Cycles" by Kornilov, Boine-Frankenheim and Ondreka (July 2013) [1] two different scenarios are studied. Both are starting with the proton manipulations at injection energy of 4 GeV (kinetic) and accelerate within 650 ms to 29 GeV. However, they differ in the transition handling:

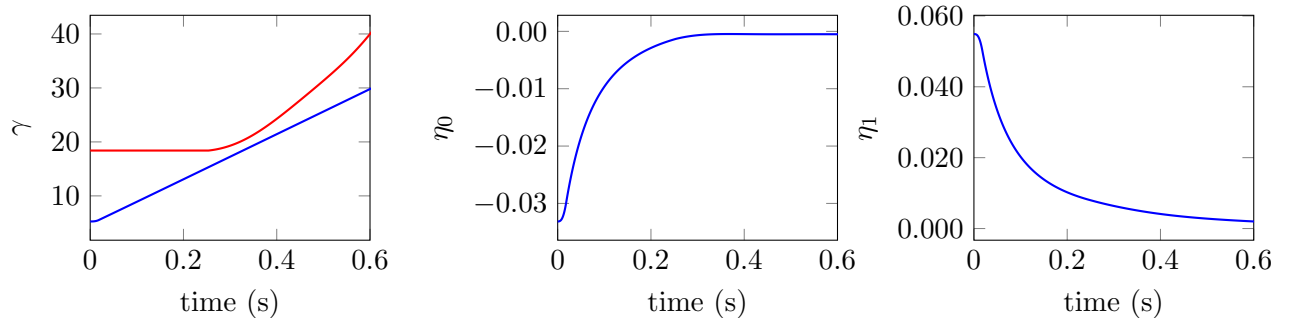
1. **(Fast / Smooth) γ_t shift:** The lattice used for the first 240 ms has $\gamma_t = 18.3$. After 240 ms the optics will be changed to $\gamma_t = 45.5$, such that the beam always stays below transition during acceleration—[2]. The corresponding Lorentz and phase slip factors are shown in Fig. 1. The fast lattice change can, however, cause a mismatch if the acceleration ramp is not adjusted properly. The parameters of a lattice with a smooth shift in γ_t studied in [3] is shown in Fig. 2 and discussed in Sec. 2.



(a) Acceleration ramp (blue) and γ_t (red)

(b) Phase slip factor

Figure 1: Parameters for scenario 1 with fast γ_t shift



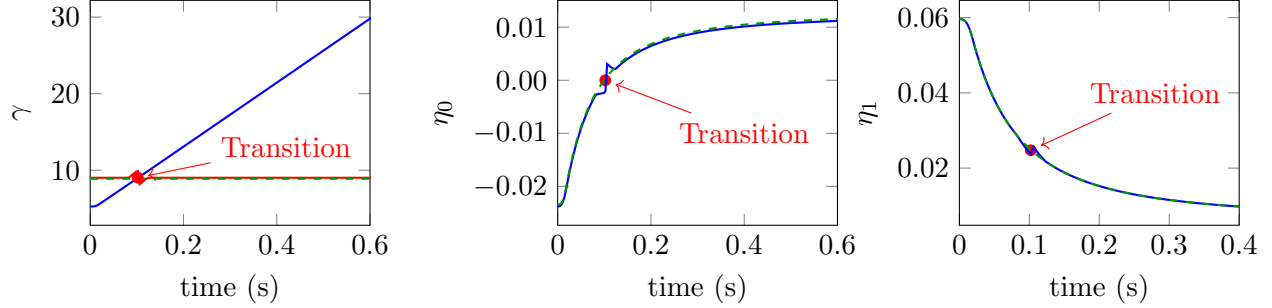
(a) Acceleration ramp (blue) and γ_t (red)

(b) Phase slip factor

(c) Second order phase slip factor

Figure 2: Parameters for scenario 1 with smooth γ_t shift

2. **Transition crossing / jump:** The lattice has $\gamma_t = 8.9$ during the complete acceleration. This leads to a transition crossing along the acceleration ramp. Fig. 3 shows the Lorentz and phase slip factors. The simulations are discussed in Sec. 3. In the case of a γ_t jump, the phase slip factors are briefly modified around transition. Why such a jump is used and the corresponding parameters are discussed in Sec. 5.



(a) Acceleration ramp (blue) and γ_t (red with and green without jump) (b) Phase slip factor (blue with and green without jump) (c) Second order phase slip factor (blue with and green without jump)

Figure 3: Parameters for scenario 2: transition crossing / jump

In the SIS100 proton cycle prior to the acceleration ramp bunch manipulations take place to merge four injected bunches to one [4]. The manipulations result in a bunch distribution which properties are listed in Tab. 1. For a maximum bucket area, the RF voltage amplitude at harmonic number $h = 5$ should be as high as possible, i.e. 280 keV, with a synchronous phase of 30.46 deg on the ramp. However, the matched rms momentum spread of 2.6×10^{-3} for the initial emittance already exceeds the maximum momentum spread during the ramp without considering a possible increase due to the non-adiabatic behavior near transition. Therefore, the RF voltage amplitude is reduced to 190 keV and a synchronous phase of 48.34 deg ensures the same energy ramp. For simulations presented in this report a simplified acceleration ramp with fixed RF voltage amplitude and synchronous phase at harmonic number $h = 5$ is used (see Tab. 2). The constraints on the longitudinal phase space during the ramp and at final energy are given in Tab. 3.

Table 1: Initial parameters of proton beam after longitudinal manipulations

Parameter	Value
Kinetic Energy	4 GeV
Intensity	2×10^{13}
Number of bunches	1
rms bunch length	22.6 m
rms momentum spread	1.3×10^{-3}
rms emittance	0.48 eV s

Table 2: Parameters of the SIS100 acceleration ramp

Parameter	Value
Magnets ramp rate	2.5 T s^{-1}
RF voltage amplitude	280 kV
Number of cavities	14
Harmonic number	5
Synchronous phase below transition	30.46°
Synchronous phase above transition	149.54°
Energy change $\dot{\gamma}$	41.09 s^{-1}

Table 3: Parameters of the proton beam during and after acceleration

Parameter	Value
Kinetic Energy	29 GeV
Maximum particle loss during ramp	1 %
Maximum rms bunch length at final energy	$25 \text{ ns} \hat{=} 7.5 \text{ m}$
Maximum rms momentum spread during ramp	2.5×10^{-3}

Without intensity effects the phase space dynamics near transition energy are well known in theory [5, 6, 7]. Since the synchrotron frequency ω_s depends on the phase slip factor

$$\eta_0 = \frac{1}{\gamma_t^2} - \frac{1}{\gamma^2}, \quad (1)$$

it slows down if $|\gamma_t - \gamma| \ll 1$ and the adiabaticity condition $\omega_s^{-1} |d\omega_s/dt| \ll 1$ is not satisfied anymore. This results in a non-adiabatic synchrotron motion in a region near transition given by the nonadiabatic time [5]

$$T_c = \left(\frac{\beta_t^2 \gamma_t^4 |\tan \varphi_s|}{2\omega_0 h \dot{\gamma}^2} \right)^{1/3} \quad (2)$$

with the synchronous phase φ_s and the revolution frequency ω_0 . A second effect on the synchrotron motion arises from the nonlinearities in the phase slip factor. Due to the high-order components of the momentum compaction factor, the phase slip factor is in general momentum spread dependent, i.e. the phase slip factor of different particles changes its sign at different times. To characterize this effect, the nonlinear time

$$T_{nl} = \frac{\gamma_t \alpha_1 \delta_{\max}}{2\dot{\gamma}} \quad (3)$$

with $\alpha_1 = \eta_1 \gamma_t^2$ assuming $\alpha_1 = 2$ [1] can be defined as the difference between the time when the phase slip factor for the synchronous particle and for the particle with momentum spread δ_{\max} changes sign. The emittance growth due to chromatic nonlinearities was first described by Johnsen [8]. It can be estimated by [9]

$$\frac{\Delta S}{S} \approx 0.76 \frac{T_{nl}}{T_c} \quad (4)$$

with the rms bunch area S if $T_{nl} \ll T_c$.

The presented simulations are done by a self-written longitudinal PIC code based on the tracking equations

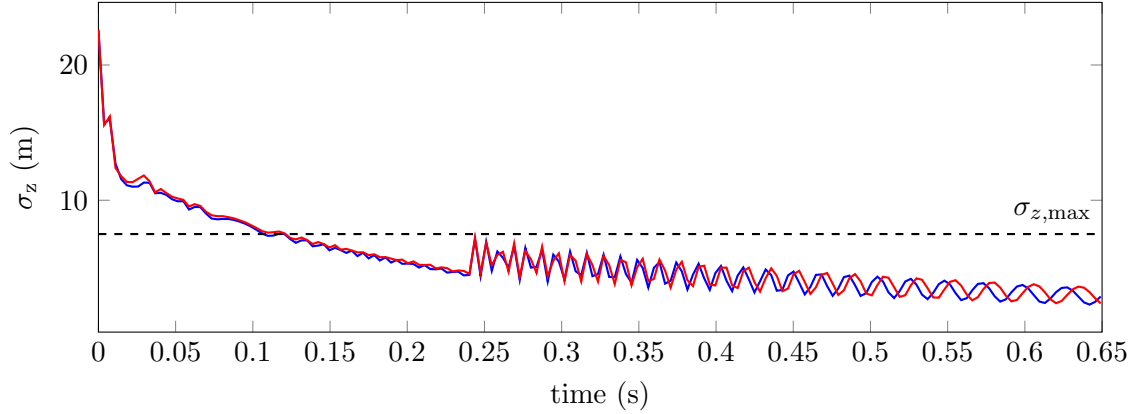
$$\delta_j^{n+1} = \delta_j^n + \frac{q}{\beta_0^2 E_0} V(z_j^n) \quad (5)$$

$$z_j^{n+1} = z_j^n - C\eta(\delta_j^{n+1})\delta_j^{n+1}, \quad (6)$$

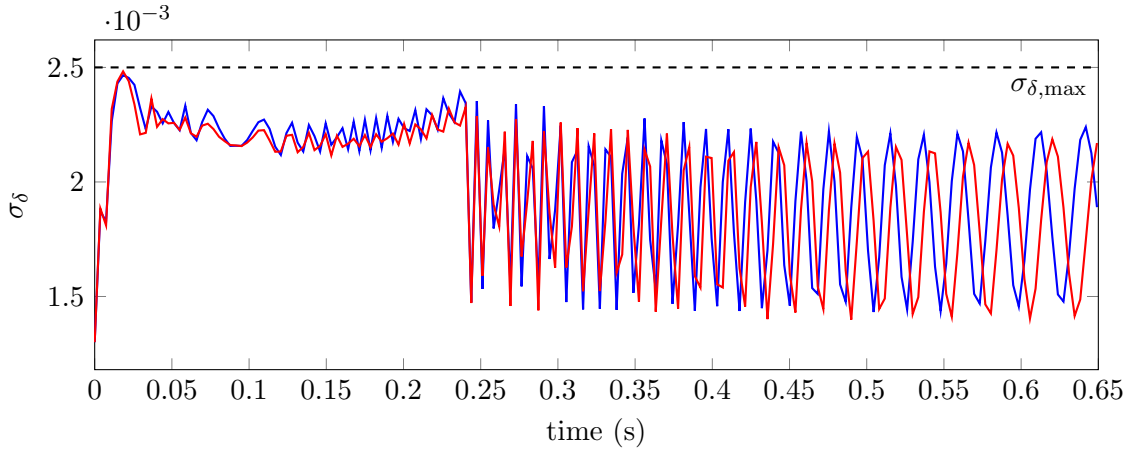
where the first order phase slip factor is included by $\eta(\delta) = \eta_0 + \eta_1\delta$, β_0 and $E_0 = \gamma_0 mc^2$ are speed and energy of the synchronous particle, respectively, and the voltage potential $V(z_j^n)$ is given as a sum of the rf potential and the space charge potential.

2 Acceleration without transition crossing: γ_t shift

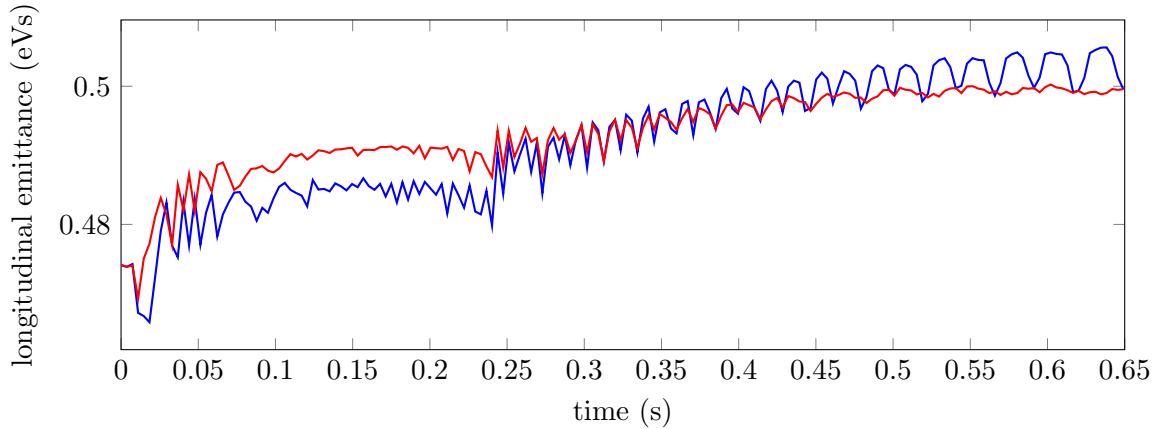
To avoid transition crossing during the acceleration ramp, the first scenario includes additional magnets in the SIS100 lattice used to increase the transition energy within the cycle. In the simulations the lattice change is implemented as a discontinuous phase slip factor (see Fig. 1b). The initial distribution is tracked through the acceleration ramp lasting for 650 ms or 179000 turns and the resulting statistics are plotted in Fig. 4. This shows that the longitudinal emittance is almost conserved during acceleration and the distribution meets the requirements for the accelerated SIS100 bunch (see Tab. 3). However, the sudden change of transition energy leads to a mismatch and therefore oscillations in the longitudinal phase space larger than the effect of space charge on



(a) RMS bunch length



(b) RMS momentum spread



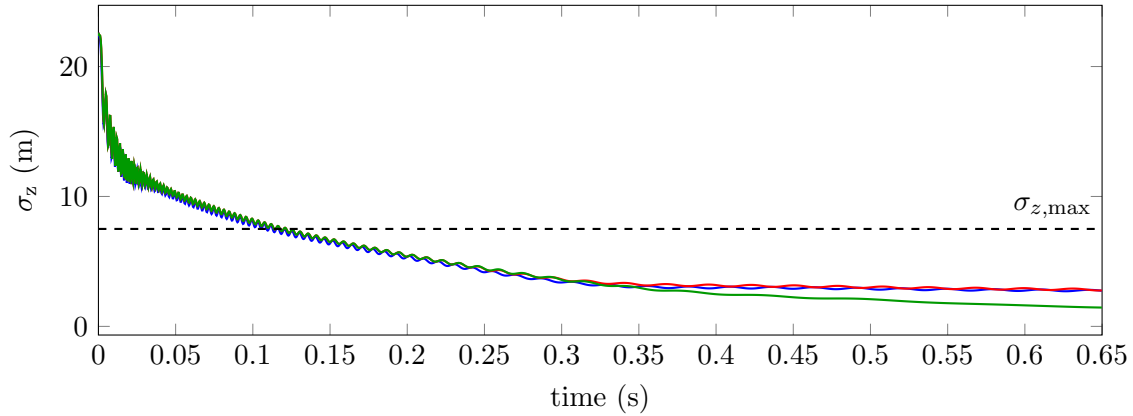
(c) Longitudinal rms emittance

Figure 4: Statistics for scenario 1 with fast γ_t increase leading to a mismatch in the bunch distribution. Results of simulations with parameters plotted in Fig. 1 are shown in blue and red without and with space charge, respectively.

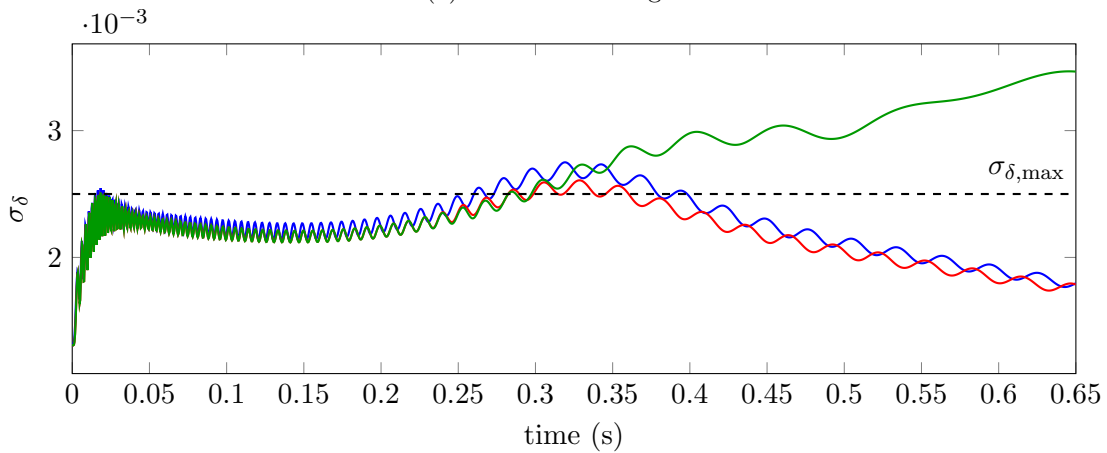
the bunch distribution. A more suitable acceleration ramp would probably allow the distribution in phase space to be matched to the requirements after the lattice change so that the oscillations are avoided.

Another option for better matching is a smooth change of the transition energy along the acceleration ramp (cf. Fig. 2). This was proposed by S. Sorge in 2012 [3]. It causes no additional oscillations during acceleration and leads to an almost perfect longitudinal emittance conversation (see Fig. 5). Only small quadrupolar oscillations due to a small mismatch at the beginning of acceleration remains during the ramp. A better chosen RF voltage ramp at the beginning or a longitudinal feedback system [10] could cure that.

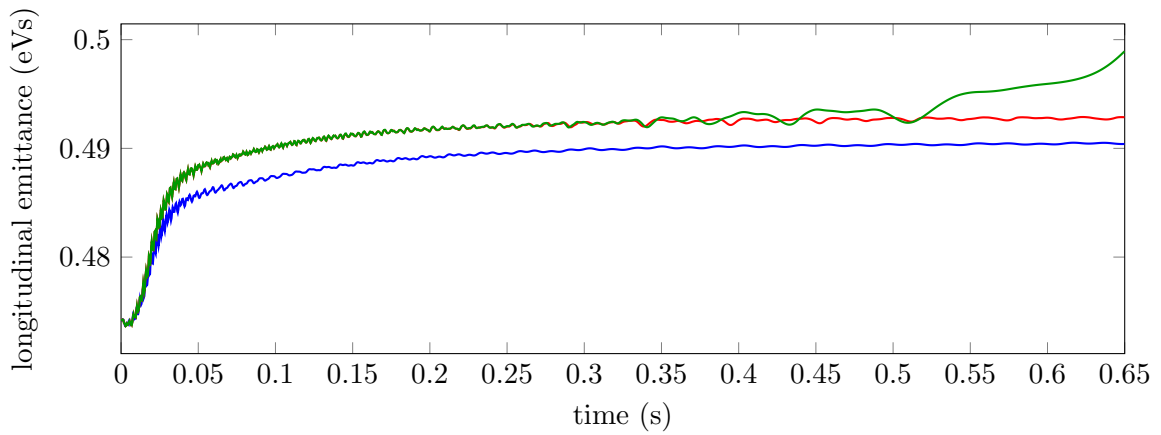
Although the proposed parameters provide a suitable longitudinal phase space at flat-top, reducing the proposed increase in transition energy would lead to a smaller bunch length but larger momentum spread at extraction energy. The minimum bunch length is limited by the momentum acceptance during the ramp. At the same time, enough distance between the energy of the synchronous particle and the transition energy has to be kept to avoid an emittance blow-up due to nonlinear dynamics. A trade-off between minimum bunch length, minimum emittance growth and keeping the momentum acceptance is found in simulations by varying the time dependent function of the transition energy (cf. Fig. 6). This results in a bunch with $\sigma_z \approx 1.4 \text{ m} = 5 \text{ ns}$ and $\sigma_\delta \approx 4.5 \times 10^{-3}$ at flat-top (see green curves in Fig. 5 and phase space in Fig 7. The asymmetric bunch shape in momentum spread indicates that the beam dynamics are located in the alpha bucket regime since the zero order phase slip factor is very close to zero (cf. [11]).



(a) RMS bunch length

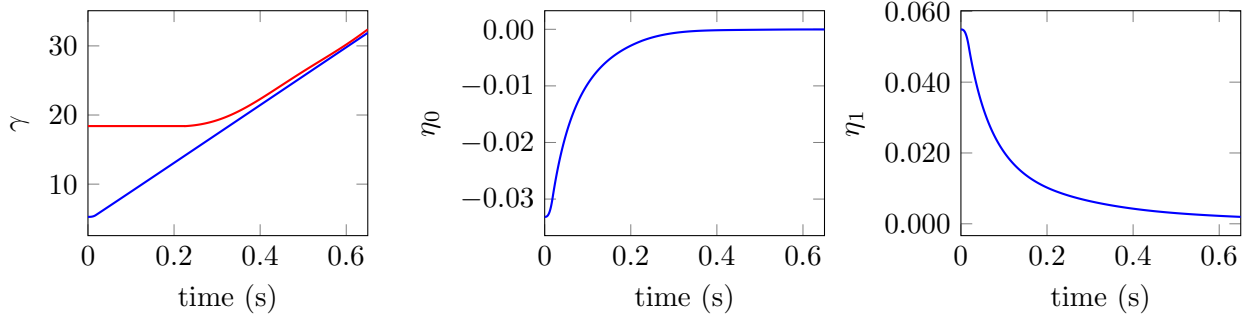


(b) RMS momentum spread



(c) Longitudinal rms emittance

Figure 5: Statistics for scenario 1 with smooth γ_t increase. Results of simulations with parameters plotted in Fig. 2 are shown in blue and red without and with space charge, respectively. The green curves shows the statistics for minimal bunch length by keeping transition energy as low as possible (cf. Fig. 6).



(a) Acceleration ramp (blue) and γ_t (red)

(b) Phase slip factor

(c) Second order phase slip factor

Figure 6: Parameters for scenario 1 with smooth γ_t increase but keeping transition energy as low as possible for minimal bunch length

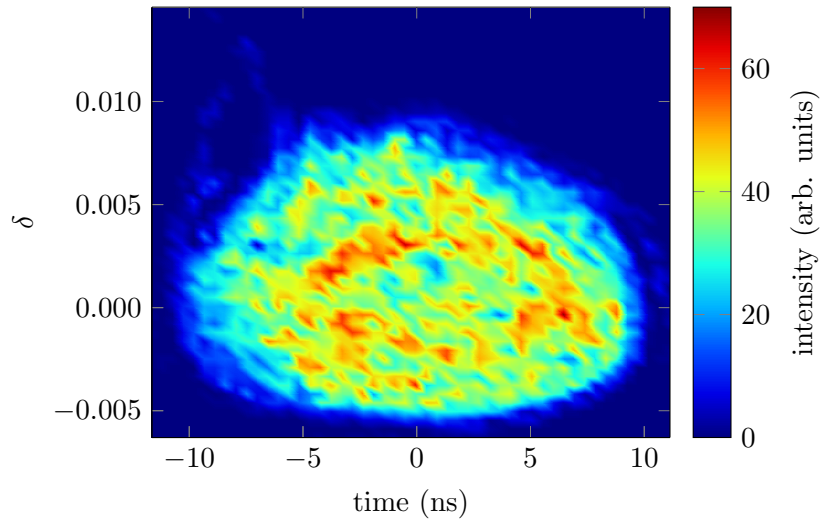
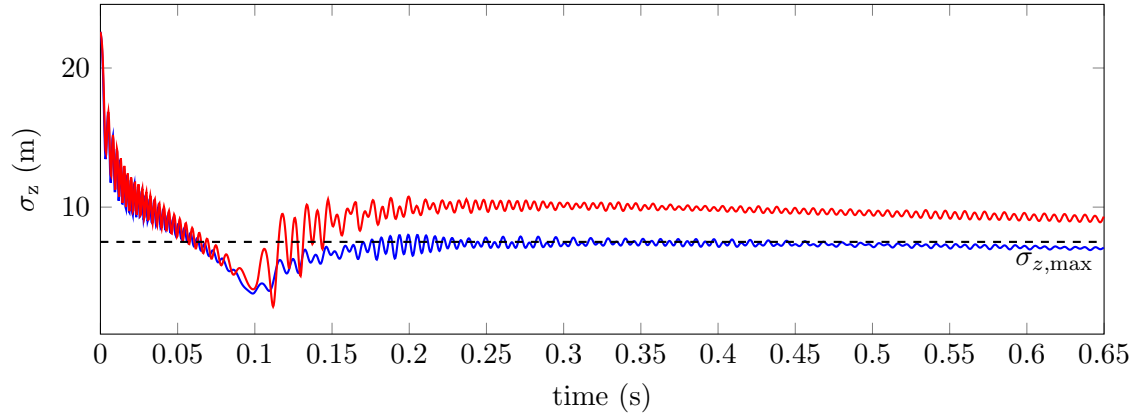


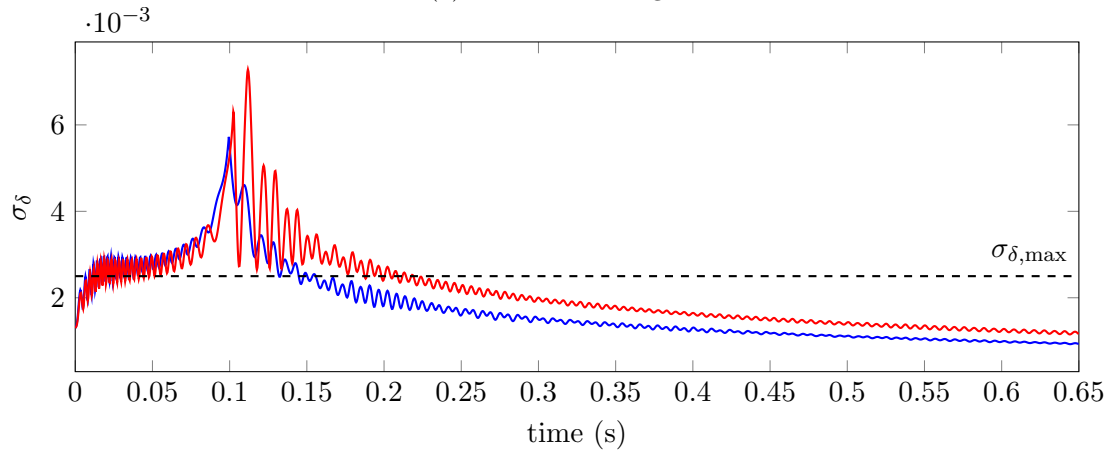
Figure 7: Phase space at the end of the acceleration ramp for scenario 1 with smooth γ_t increase but keeping transition energy as low as possible for minimal bunch length (cf. parameters in Fig. 6 and statistics in Fig. 5). The asymmetry in momentum spread indicates that the dynamics are located in the alpha bucket regime [11].

3 Transition crossing

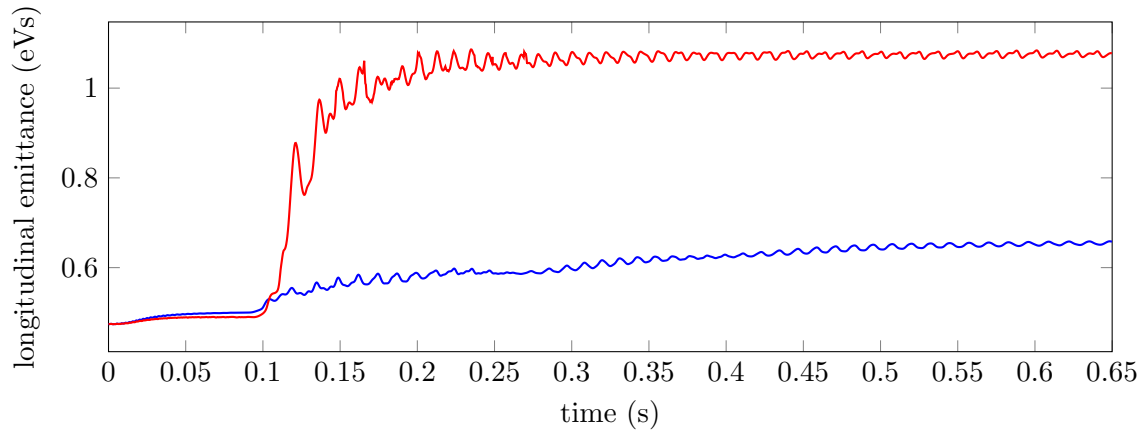
The second scenario would omit additional magnets, but contains a transition crossing after 102 ms (see Fig. 3). Fig. 8 shows the bunch length, momentum spread and longitudinal emittance along the ramp. As predicted in [1] the transition crossing is clearly seen by the minimum of the bunch length and maximum of the momentum spread, that even exceeds the maximum possible value without particle loss (cf. Tab. 3). The nonadiabatic time around transition crossing (see Eq. 2) is $T_c \approx 5$ ms. Within this time there is a sudden emittance growth in both simulations without and with space charge followed by a slight increase afterwards. At the extraction energy of 29 GeV the bunch distribution without space charge has a rms bunch length of $\sigma_z \approx 7.1$ m = 23.7 ns, a momentum spread of $\sigma_\delta \approx 9.3 \times 10^{-4}$ and a longitudinal emittance of $\varepsilon_z \approx 0.66$ eV s, i.e. an increase of almost 40% during the acceleration ramp – mainly caused by the transition crossing. This can be compared to the theory: With the maximum momentum spread of about $\delta_{\max} = 5 \times 10^{-3}$ the nonlinear time (Eq. 3) in this scenario is $T_{\text{nl}} \approx 1.1$ ms. The emittance growth by the Johnsen effect (Eq. 4) is thus $\Delta S/S \approx 16.7\%$ which corresponds very well to the sudden emittance growth at transition. However, with space charge the emittance at extraction additionally increases by 162% to $\varepsilon_z \approx 1.07$ eV s, the rms bunch length to $\sigma_z \approx 9.31$ m = 31 ns and the momentum spread to $\sigma_\delta \approx 11.6 \times 10^{-4}$, such that the final bunch length is larger than the maximum tolerable value (cf. Tab. 3). Furthermore, the momentum spread exceeds the maximum tolerable value slightly at the beginning of the ramp and significantly around transition, although beam loading and other impedance sources as possible candidates for additional longitudinal emittance growth are not yet included in the presented simulations. To keep the momentum spread below the limit, the acceleration ramp is modified in the next section and a jump of the transition energy is introduced in the section after next.



(a) RMS bunch length



(b) RMS momentum spread



(c) Longitudinal rms emittance

Figure 8: Statistics for scenario 2: transition crossing without any cure for possible emittance blow-up. Results of simulations with parameters plotted in Fig. 3 are shown in blue and red without and with space charge, respectively.

4 Transition crossing with modified acceleration ramp

For the previous sections the acceleration ramp is chosen such that the desired energy change per turn is reached by the maximum available RF voltage amplitude resulting in the largest bucket area (cf. Tab. 2). However, the matched momentum spread for the given initial emittance in the transition crossing scenario (see Fig. 3) is $\sigma_\delta = 2.6 \times 10^{-3}$, i.e., above the limit given in Tab. 2. If the RF voltage amplitude is decreased and the synchronous phase is increased simultaneously to gain the desired energy per turn (see Fig. 9), the matched momentum spread also decreases. As new initial ramp parameters a RF voltage amplitude of 190 kV and a synchronous phase of 48.35° are used resulting in a matched momentum spread of $\sigma_\delta = 2.17 \times 10^{-3}$ well below the maximum value but at the same time in a bucket area which is large enough to accelerate the bunch without particle loss.

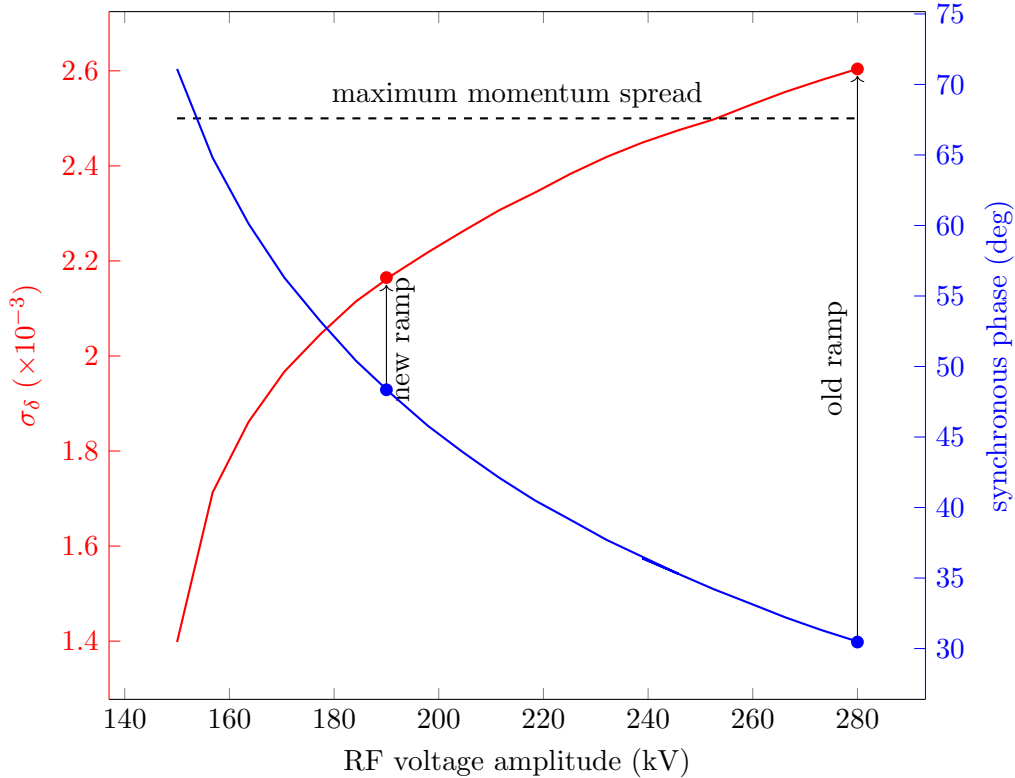


Figure 9: Synchronous phase (blue) and matched momentum spread (red) for a given RF voltage amplitude to match the initial longitudinal emittance and energy change per turn (cf. Tabs. 1 and 2)

The simulation results with the modified RF voltage and synchronous phase are shown in Fig. 11. As expected, the momentum spread stays below the maximum value before transition crossing. However, the momentum spread exceeds the limit near to transition, the final bunch length is too large, especially with space charge, and there is still a significant emittance growth at transition in the simulation with space charge. With a linearly increasing RF voltage amplitude up to 280 kV and a accordingly decreasing synchronous phase, the final bunch length is almost exactly at the maximum value but of course this can not prevent the peak in momentum spread and the emittance growth at transition. Therefore, a γ_t jump is necessary.

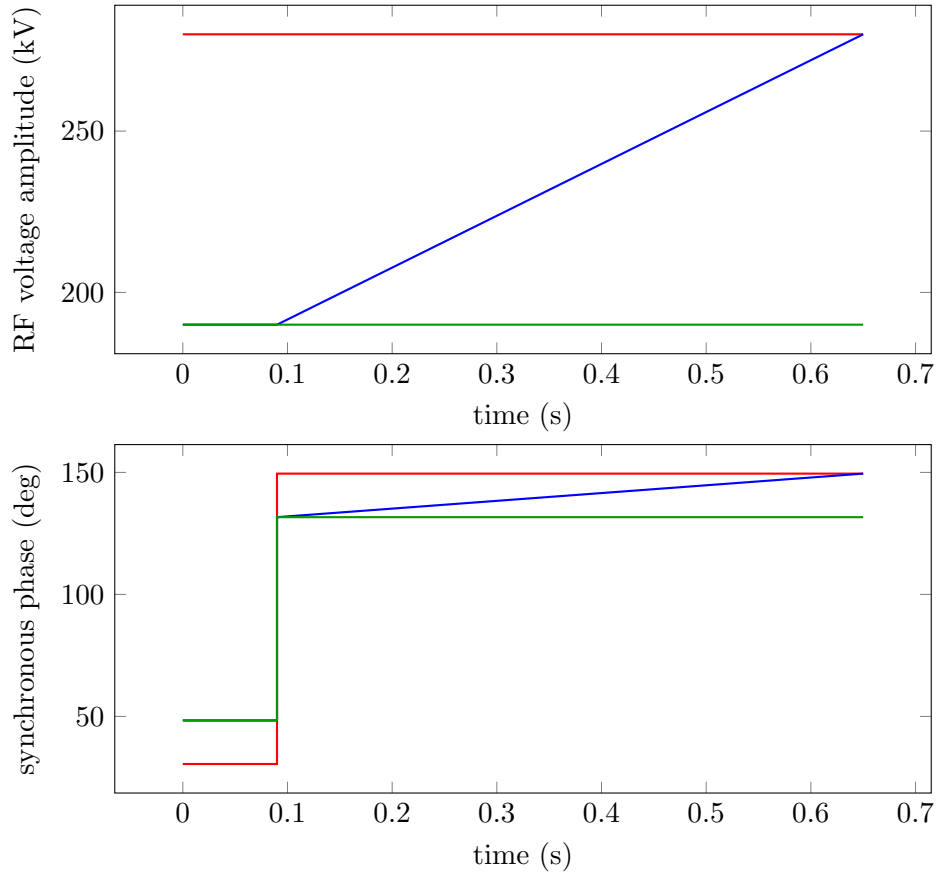
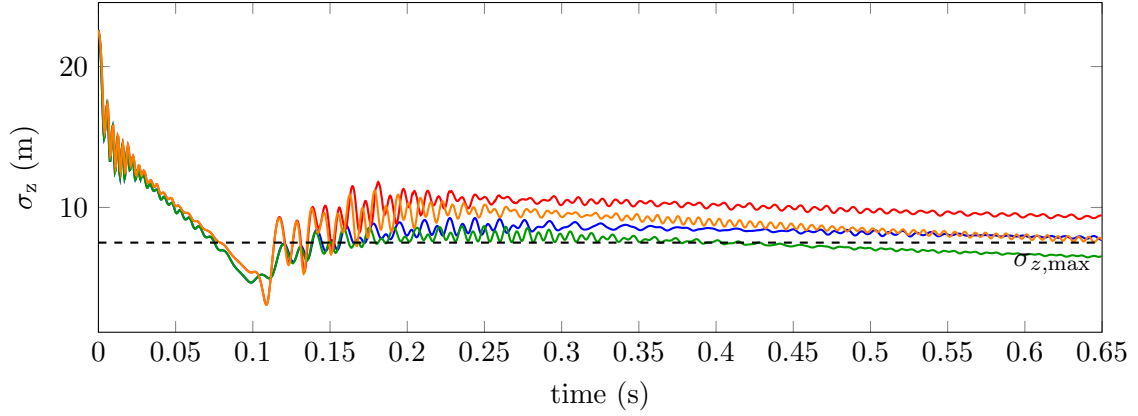
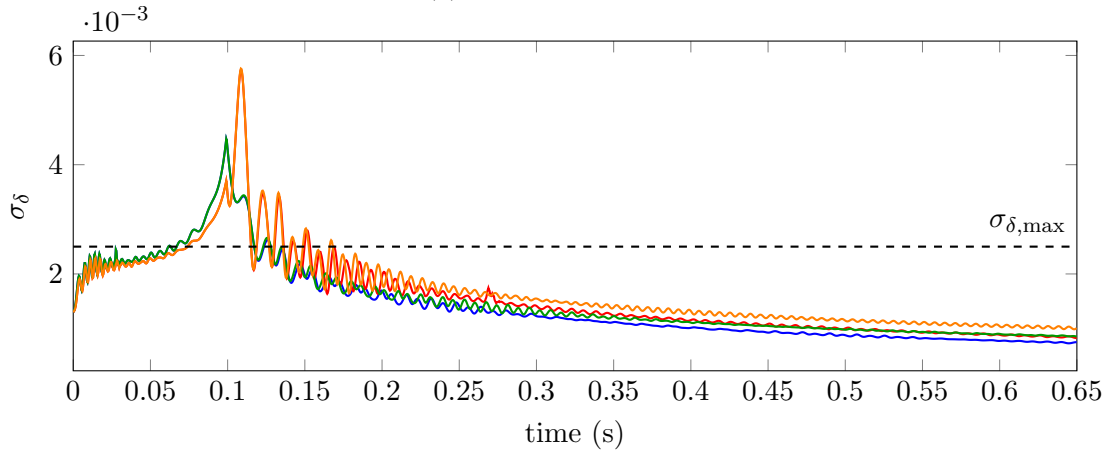


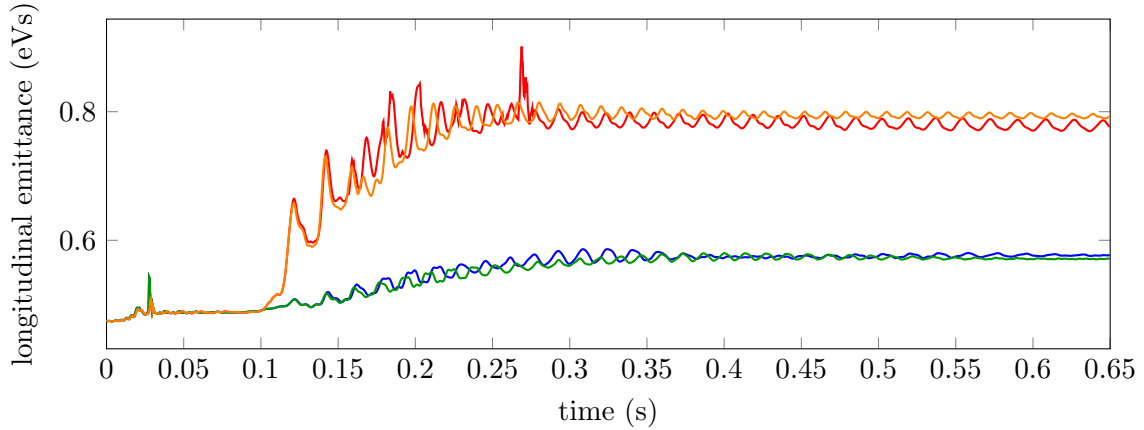
Figure 10: RF voltage amplitude (top) and synchronous phase (bottom) of the different ramps: the initial ramp with constant amplitude and phase (red), the modified ramp with decreased but constant amplitude and increased but constant phase (blue) and the mixed one with constant amplitude and phase below transition and linearly changing parameters above transition (green).



(a) RMS bunch length



(b) RMS momentum spread



(c) Longitudinal rms emittance

Figure 11: Statistics for scenario 2 with modified acceleration ramp: transition crossing without any cure for possible emittance blow-up. Results of simulations with parameters plotted in Fig. 3, 190 kV RF amplitude and a synchronous phase of 48.35° are shown in blue and red without and with space charge, respectively. The green (without space charge) and orange (with space charge) lines show the simulation results if the RF voltage amplitude increases linearly to 280 kV after transition and the synchronous phase decreases accordingly.

5 Transition crossing with γ_t jump

Crossing transition at planned SIS100 intensity leads to a not tolerable emittance growth and bunch lengthening due to nonlinear effects and space charge. To prevent this, a jump of the transition energy in the range of the nonadiabatic time can be introduced. For this, the transition energy is increased before the particle energy reaches transition, rapidly decreased below the initial transition energy and then again increased to stay at the initial transition energy for the remaining acceleration above transition. Fig. 12 shows an example of such a γ_t jump. The jump can be described by a shift Δt_{shift} with respect to the original transition crossing, the length Δt_{jump} between maximum and minimum of γ_t , the values $\Delta\gamma_{t,\text{up/down}}$ of these two extrema and the increasing and decreasing slopes Δt_{slope} in front of the maximum and after the minimum.

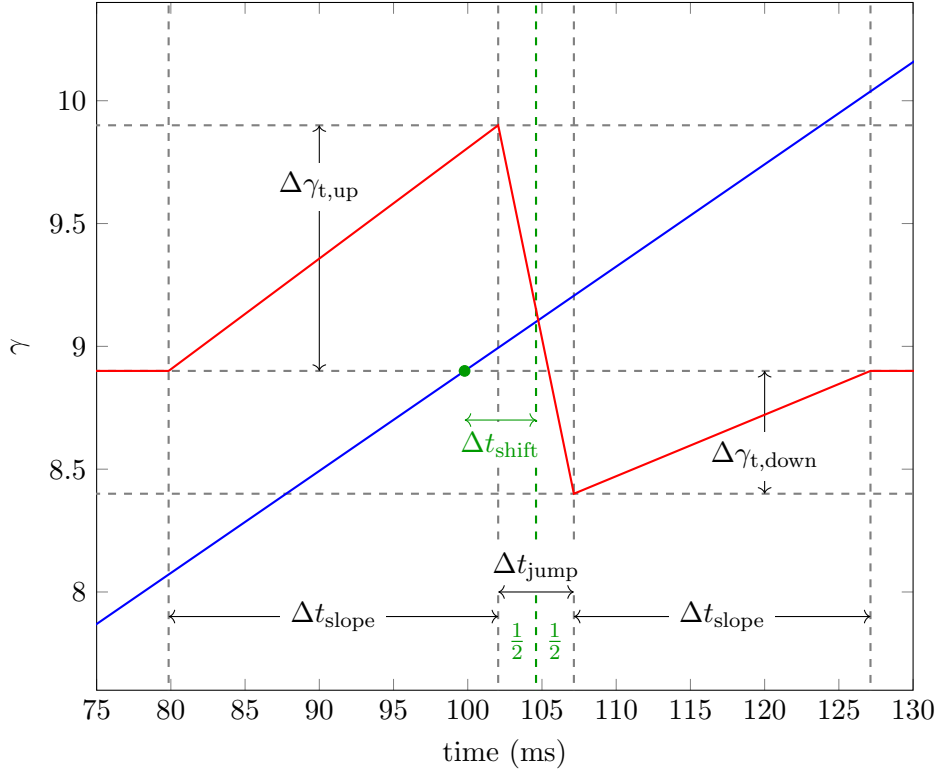


Figure 12: Jump of the transition energy around transition crossing

In the following, the emittance growth caused by the γ_t jump, the maximum momentum spread (during the jump) and the final bunch length after the ramp are studied by varying these jump parameters.

For fixed $\Delta t_{\text{slope}} = 20.1$ ms the emittance growth $\varepsilon_z/\varepsilon_{z,0}$ varying the other parameters is plotted in Fig. 13. It can be seen that the emittance growth is always minimal for the smallest. The minimum in all simulations is reached for $\Delta\gamma_{t,\text{up}} = 2 \cdot \Delta\gamma_{t,\text{down}} = 1$ and a jump shift of 0.7 ms. This asymmetric behavior avoids a mismatch in beam size due to the change of the focusing properties of space charge at transition. Below transition the equilibrium bunch length with space charge is larger than without and above transition it is the other way around. Therefore, a symmetric jump leads to quadrupolar oscillations, whereas with an asymmetric one it is possible to jump back to a matching equilibrium bunch length (cf. Figs 3 & 4 in [12]). However, the simulations with these optimal jump parameters for minimal emittance growth, are not the optimum with regard to the maximum

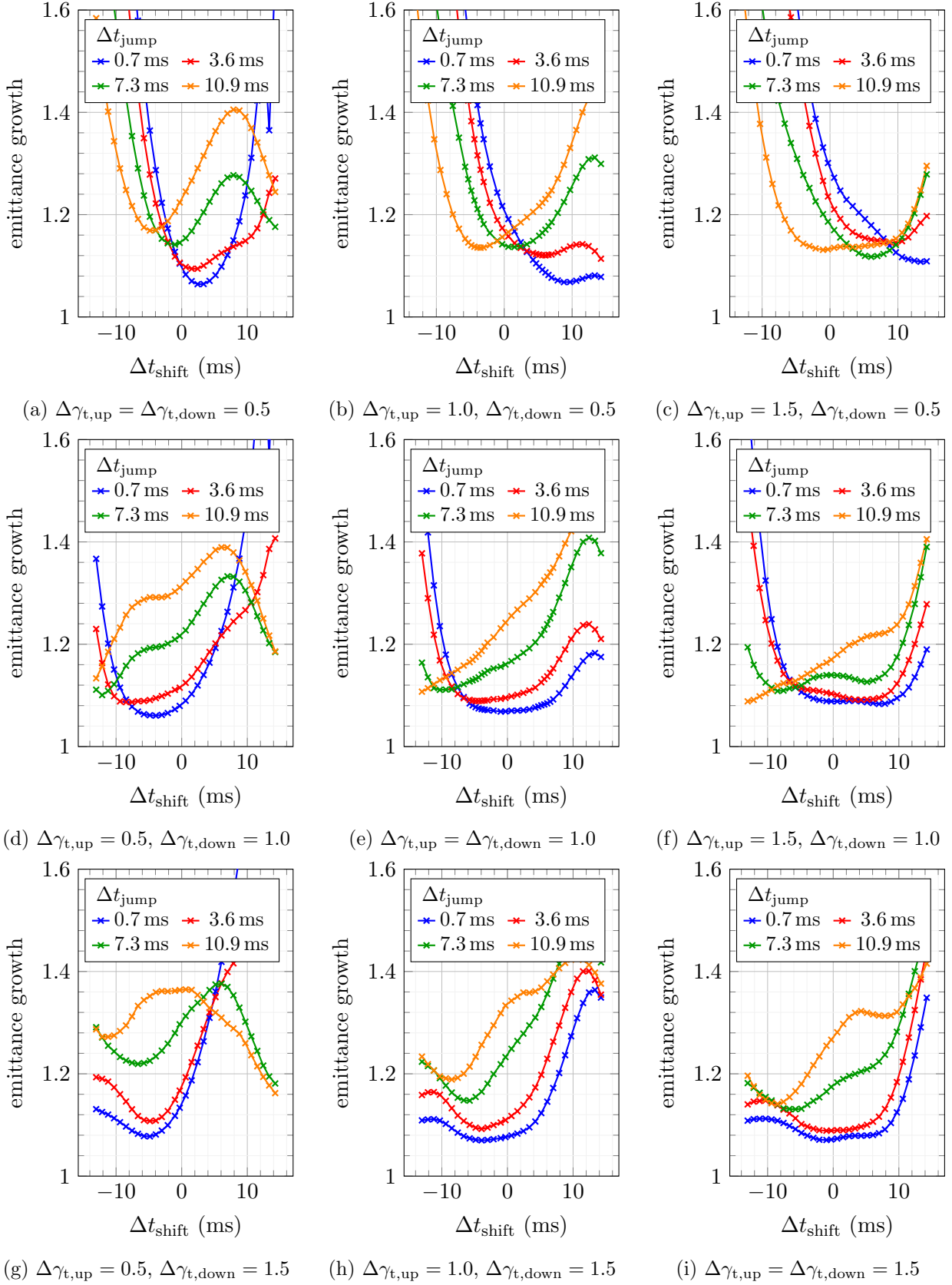


Figure 13: Emittance growth as function of different jump parameters

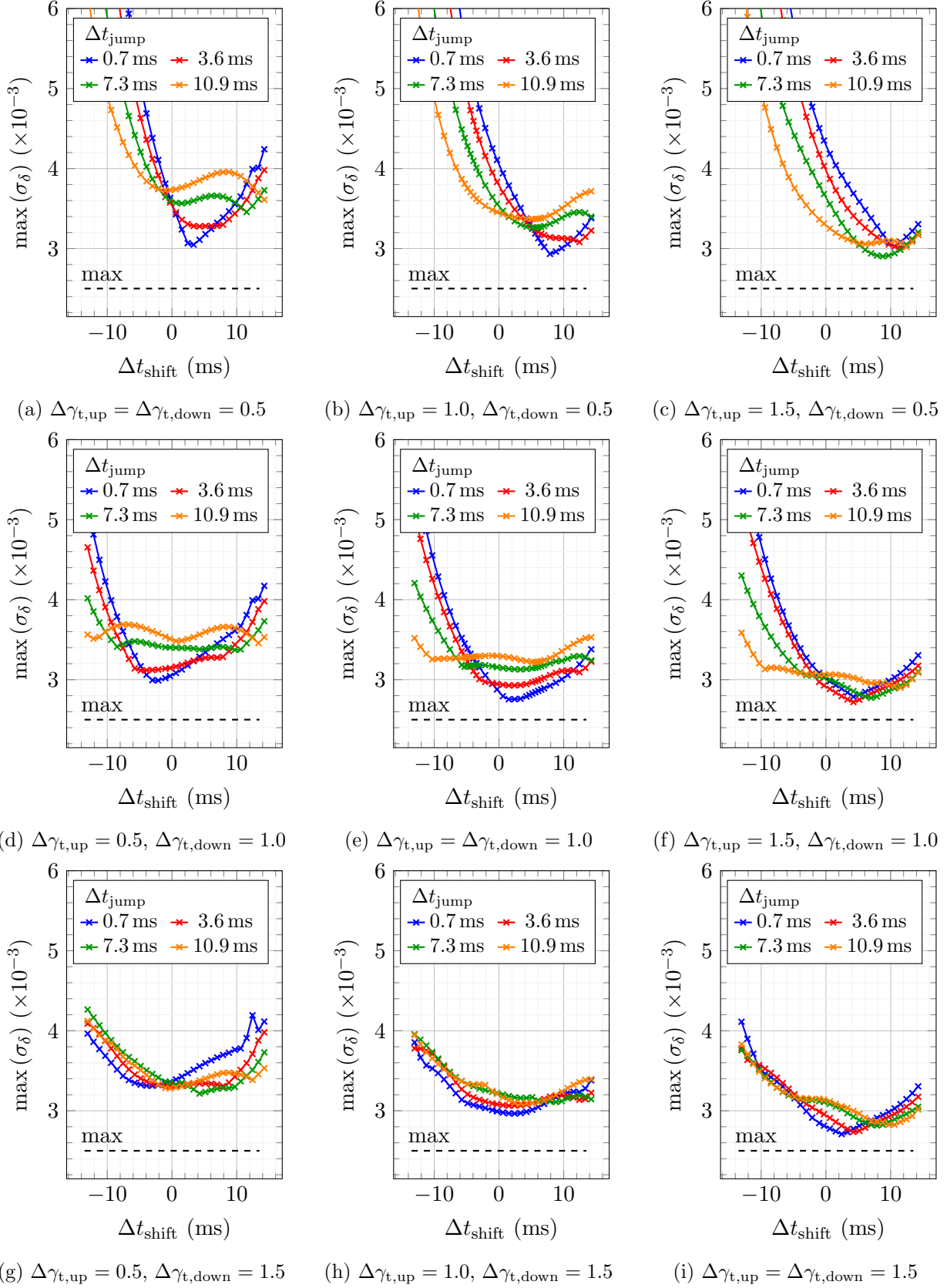


Figure 14: Maximum momentum spread as function of different jump parameters

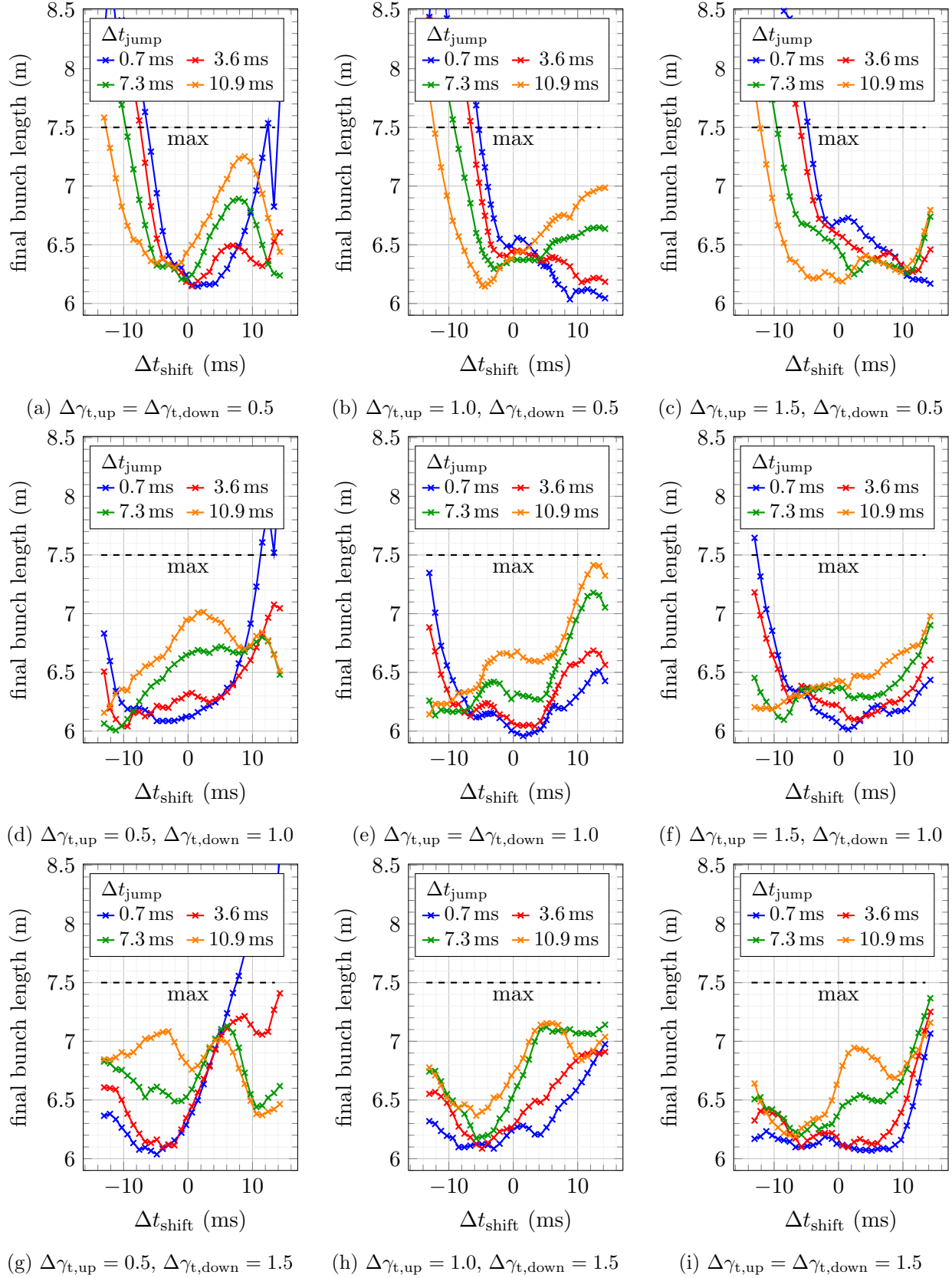


Figure 15: Final bunch length as function of different jump parameters

momentum spread (see Fig. 14). There, the symmetric jumps with $\Delta\gamma_{t,\text{up}} = 2 \cdot \Delta\gamma_{t,\text{down}} = 1$ and $\Delta\gamma_{t,\text{up}} = \Delta\gamma_{t,\text{down}} = 1.5$ result in a lower maximum momentum spread near to the desired maximum value (dashed black line in the plots). Last but not least the minimum of the final bunch length (shown in Fig. 15) justifies the symmetric jump with $\Delta\gamma_{t,\text{up}} = \Delta\gamma_{t,\text{down}} = 1$ as the optimum choice with an emittance growth around 7%, a bunch length below 6 m and a maximum momentum spread of 0.027×10^{-3} . Note that the final bunch length of almost all simulations is below the maximum tolerable value.

Similar to the discussion of transition crossing without jump (cf. Sec. 3) theoretical requirements on the γ_t jump can be formulated by the emittance growth due to the nonlinear Johnson effect [9]. To compensate this chromatic nonlinear effect the minimum jump size is given by $\Delta\gamma_t > 2\dot{\gamma}T_{\text{nl}} \approx 0.05$ which is fulfilled in any case. The minimum speed $|\dot{\gamma}_t|$ of the γ_t jump is

$$\frac{|\dot{\gamma} - \dot{\gamma}_t|}{\dot{\gamma}} > \left(0.76 \frac{S}{\Delta S} \frac{T_{\text{nl}}}{T_c}\right)^{6/5}. \quad (7)$$

This can be reformulated as constraint on Δt_{jump} by

$$\Delta t_{\text{jump}} < \frac{\Delta\gamma_t}{\dot{\gamma} \left\{1 - \left(0.76 \frac{S}{\Delta S} \frac{T_{\text{nl}}}{T_c}\right)^{6/5}\right\}} \quad (8)$$

and plotted in Fig. 16 for $\Delta\gamma_t = -(\Delta\gamma_{t,\text{up}} + \Delta\gamma_{t,\text{down}}) = -2$.

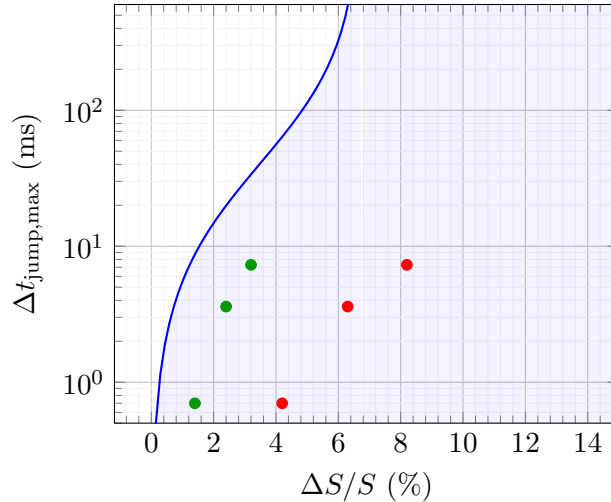


Figure 16: Maximum jump length for a maximum allowable fractional growth of bunch area from theory Eq. 8 (blue line) and simulated jump lengths measured directly after the jump (green) and at the end of the ramp (red)

Comparing the simulation results shown as red dots in the plot (only emittance growth at and after transition) and the theoretical limit by the nonlinear effects. The emittance growth in the simulations is much larger than the theoretical limit since nonadiabatic effects on the ramp after transition – maybe caused oscillations due to a mismatch right after transition – lead to much larger emittance blow-up than directly at transition with a continued growth along the ramp (cf. Fig. 18c).

Furthermore, the already varied parameters are now chosen as fixed at the optimum and Δt_{slope} is varied. The simulation results plotted in Fig. 17 show a slightly smaller maximum momentum

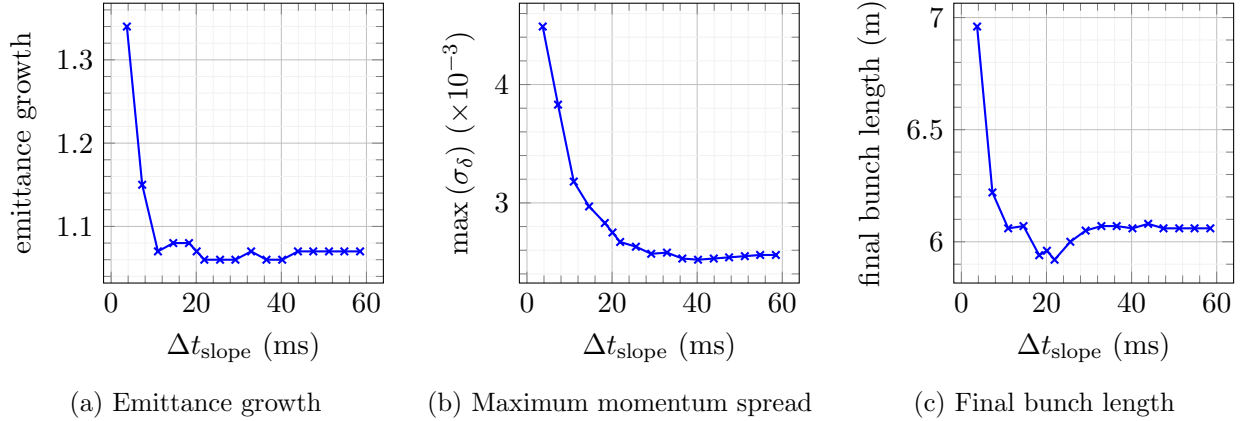


Figure 17: Emittance, momentum spread and bunch length as a function of the length of the slopes before and after the γ_t jump for $\Delta\gamma_{t,\text{up}} = \Delta\gamma_{t,\text{down}} = 1.0$, $\Delta t_{\text{jump}} = 0.7$ ms and $\Delta t_{\text{shift}} = 0$ s.

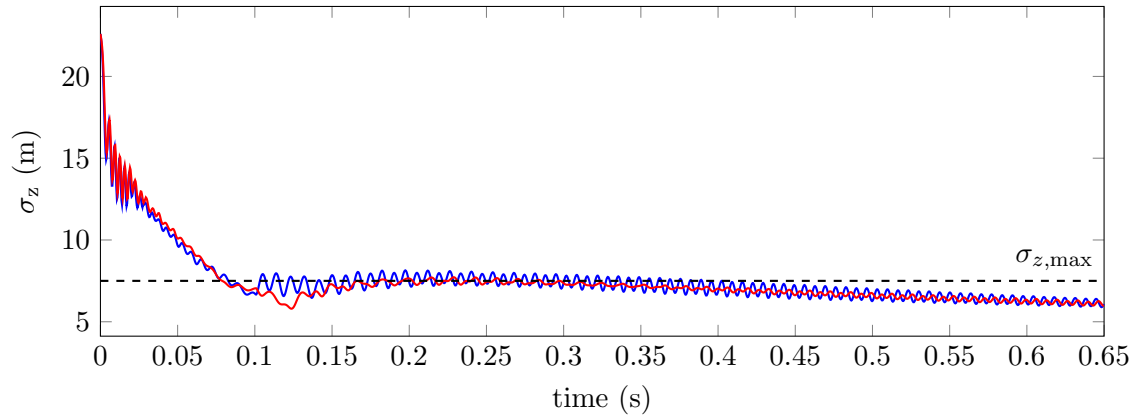
spread at about $\Delta t_{\text{slope}} = 40$ ms then at the prior used $\Delta t_{\text{slope}} = 20.1$ ms. Although this is only a small improvement, extending the length of the slope can be used to bring the maximum momentum spread near to the desired limit.

Fig. 18 summarizes the statistics for the acceleration ramp with minimum emittance growth due to transition crossing. The proton bunch has a final length of $\sigma_z \approx 6.06$ m, a momentum spread of $\sigma_\delta \approx 8.1 \times 10^{-4}$ and a longitudinal emittance of $\varepsilon_z \approx 0.504$ eVs. However, there is an emittance growth of about 3% at the beginning of the acceleration ramp which can be reduced by a more complex ramp than used for these simulations and an emittance growth of about 5% occurs during and after transition. If the number of particles in the bunch is lower, the asymmetry in the timing of the γ_t jump has to be adapted to the new intensity. Thus, the simulation without space charge effects but with the same jump parameters shows a larger emittance growth after transition crossing due to the mismatch at the γ_t jump (blue curve in Fig. 18c).

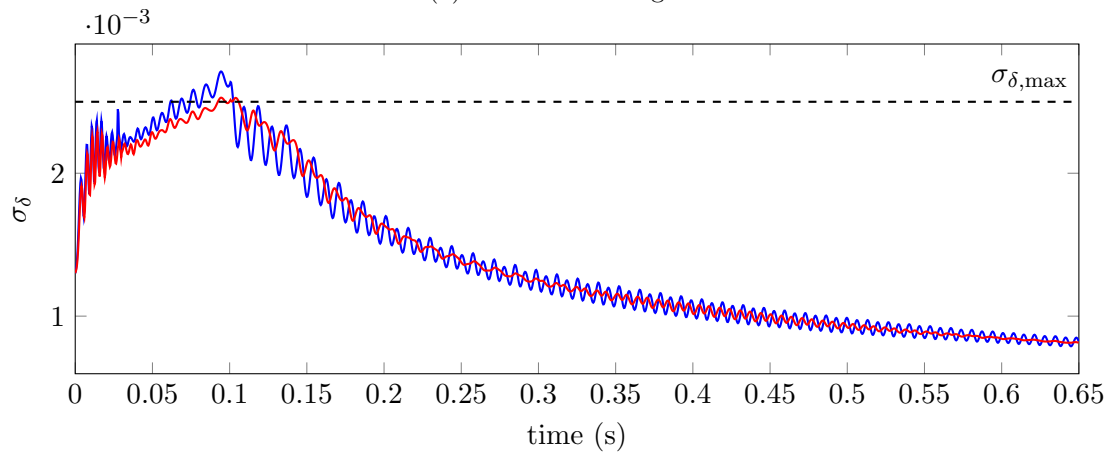
To conclude, the best jump parameters are summarized in Tab 4 and the phase space after acceleration is plotted in Fig. 19.

Table 4: γ_t jump parameters with minimal emittance growth at nominal intensity of 2×10^{13} particles

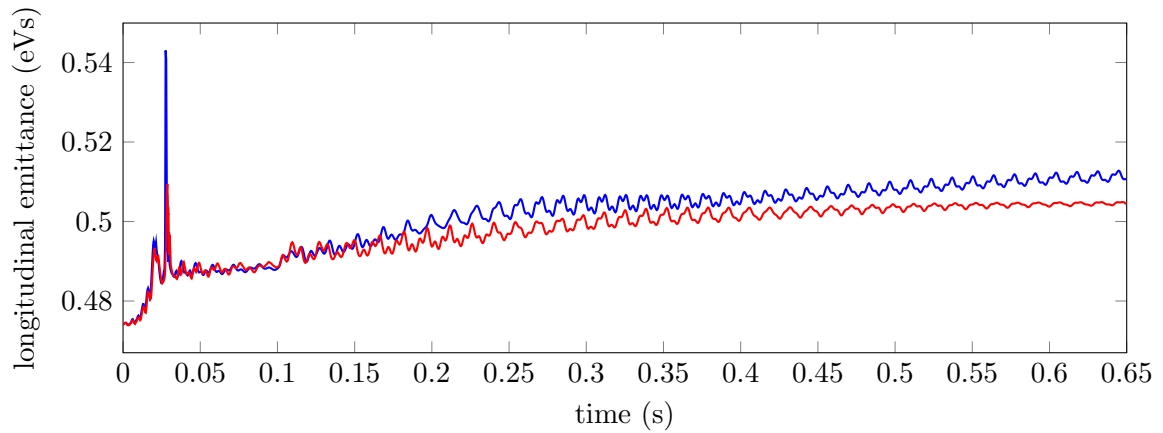
Parameter	Value (in turns)	Value in ms
$\Delta\gamma_{t,\text{up}}$	1.0	–
$\Delta\gamma_{t,\text{down}}$	1.0	–
Δt_{slope}	11000	40.2
Δt_{jump}	200	0.7
Δt_{shift}	400	1.4



(a) RMS bunch length



(b) RMS momentum spread



(c) Longitudinal rms emittance

Figure 18: Statistics for scenario 2 with γ_t jump and modified acceleration ramp (with and without space charge in red and blue, respectively)

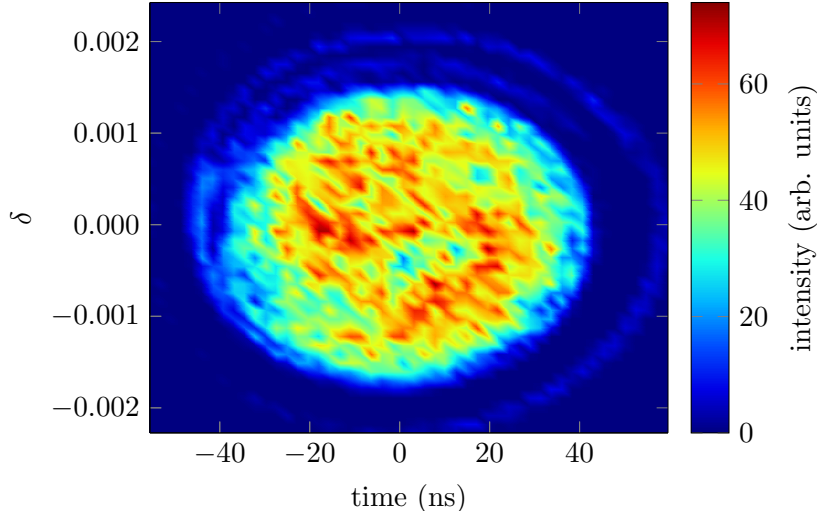


Figure 19: Phase space at the end of the acceleration ramp for scenario 2 with γ_t jump and with space charge for the parameters shown in Tab. 4

6 Conclusion and Outlook

The SIS100 proton cycle accelerates protons from 4 GeV to 29 GeV. The proposed lattice design requires taking care of the beam dynamics around transition energy. For this, two different scenarios are foreseen: Shifting transition energy during the acceleration ramp to avoid transition crossing and crossing transition with a γ_t jump to control the possible blow-up in phase space.

The longitudinal simulations presented in this report have shown that shifting the transition energy during the ramp – especially if this is done smoothly – would lead to a bunch distribution fulfilling all requirements (cf. Tab. 3). For the implementation, however, the transition energy has to be increased above $\gamma_t = 40$.

For the scenario with constant $\gamma_t = 8.9$, the maximum allowed momentum spread of $\delta_{\max} = 2\sigma_{\delta, \max} = 5 \times 10^{-3}$ would be exceeded near to transition energy and a not tolerable emittance blow-up caused by space charge effects would occur. To reduce this emittance growth significantly a γ_t jump is introduced and the parameters of this jump were optimized at SIS100 nominal intensity of 2×10^{13} particles per bunch (cf. Tab. 4). This optimization results in a γ_t jump with below 7% emittance growth due to transition crossing fulfilling the requirements on bunch length and momentum spread (cf. Tab. 3). Furthermore, the simulations indicated that the most critical requirement is the maximum momentum spread along the ramp. If this could be relaxed, the γ_t jump does not have to be as fast as suggested for example in [13]. However, only longitudinal space charge effects are included in the simulations so far. Transverse effects could also require a faster jump and have to be studied in the future.

References

- [1] V. Kornilov, O. Boine-Frankenheim, and D. Ondreka, “Overview of the Longitudinal Beam Dynamics for the SIS100 Proton Cycles,” *SIS Project Note, WP 2.8.1 SIS100 Beam Dynamics*, 2013.
- [2] R. Bär, U. Blell, O. Boine-Frankenheim, L. Bozyk, K. Blasche, J. Falenski, E. Fischer,

- E. Floch, G. Franchetti, B. Franczak, P. Forck, O. Gumenyuk, I. Hofmann, P. Hülsmann, M. Kauschke, M. Kirk, H. Klingbeil, H. G. König, A. D. Kovalenko, P. Kowina, A. Krämer, D. Krämer, M. Kumm, U. Laier, M. Mehler, J. P. Meier, G. Moritz, P. Moritz, C. Mühle, K. P. Ningel, C. Omet, I. Pschorn, N. Pyka, H. Ramakers, P. Schnizer, G. Schreiber, C. Schroeder, M. Schwickert, Y. Shim, M. Sitko, B. Skoczen, S. Sorge, P. Spiller, J. Stadlmann, A. Stafniak, K. Sugita, B. Weckenmann, and H. Welker, “FAIR Technical Design Report SIS100,” tech. rep., GSI Helmholtzzentrum für Schwerionenforschung GmbH, Darmstadt, Germany, 2008.
- [3] S. Sorge, “Beam Dynamics Study Concerning SIS-100 Proton Operation Including Space Charge Effects,” in *ICAP2012*, 2012.
- [4] Y.-S. Yuan, O. Boine-Frankenheim, T. Egenolf, and V. Kornilov, “RF manipulations of high-intensity hadron beams in SIS-100,” tech. rep., GSI Helmholtzzentrum für Schwerionenforschung GmbH, Darmstadt, Germany, 2021.
- [5] K. Y. Ng, *Physics of Intensity Dependent Beam Instabilities*. Singapore, New Jersey, London, Hong Kong: World Scientific, 2006.
- [6] S. Y. Lee, *Accelerator Physics*. Singapore, New Jersey, London, Hong Kong: World Scientific, 1999.
- [7] S. Gilardoni, D. Manglunki, and European Organization for Nuclear Research., *Fifty years of the CERN proton synchrotron. Vol. 1*. CERN, 2010.
- [8] K. Johnsen, “Effects of Non-linearities on the Phase Transition,” in *HEAAC 1956*, 1956.
- [9] A. W. Chao and M. Tigner, *Handbook of Accelerator Physics and Engineering*. Singapore: World Scientific Publishing Co. Pte. Ltd., 1999.
- [10] D. Lens and H. Klingbeil, “Stability of longitudinal bunch length feedback for heavy-ion synchrotrons,” *Physical Review Special Topics - Accelerators and Beams*, vol. 16, 3 2013.
- [11] S. Sorge, “Simulation study on beam loss in the alpha bucket regime during SIS-100 proton operation,” *Nuclear Instruments and Methods in Physics Research, Section A: Accelerators, Spectrometers, Detectors and Associated Equipment*, vol. 882, pp. 129–137, 2 2018.
- [12] E. Métral and D. Möhl, “Transition Crossing,” tech. rep.
- [13] S. Aumon, D. Ondreka, S. Sorge, and K. Gross, “Transition energy crossing in the future FAIR SIS-100 for proton operation,” in *5th International Particle Accelerator Conference IPAC2014*, JACoW, 2014.